Journal of
Materials in Life Sciences

Vol. 4 No. 1 (2025)

Full Paper

Fatty Acid Profiles Based on Their Locality in Urinary Extracellular Vesicles by Using Gas Chromatography-Mass Spectrometry

Nabila Amiszan, Fatinah Adenan, Iqbal Jalaludin*

Department of Chemistry, Faculty of Science, Universiti Teknologi Malaysia, 81310 UTM Johor Bahru, Johor, Malaysia.

Article history
Received
24 April 2025
Revised
16 May 2025
Accepted
26 May 2025
Published online
31 May 2025

*Corresponding author
muhamadiqbal.j@utm.my

Abstract

The use of fatty acids in extracellular vesicles (EVs) has been largely understudied, despite their selective characteristics, which hold potential as disease biomarkers. EVs are nanosized vesicles secreted by human cells and play key roles in intercellular communication. Although lipid profiling of EVs has shown promise in differentiating between healthy and diseased individuals, fatty acids specifically remain underexplored. Due to the fatty acids' structural simplicity and high selectivity, this study focuses on profiling the fatty acids on the EVs and optimizing the isolation method of EVs using ultracentrifugation (1-cycle and 2-cycle). The fatty acid profile was compared between the fatty acids in the urine as a control and the fatty acids found on the EVs. Optimal EVs isolation was achieved using a 2-cycle ultracentrifugation process, yielding vesicles with an average size of 131.87 nm with a standard deviation of 23.84 and significantly higher protein concentration (2.970 mg/mL, $p < 0.05$). A total of 14 fatty acid methyl esters (FAMEs) were detected, with 12 shared across all localities and four (C13, C15, C18, and C30) found to vary by sample origin. Tetracosanoic acid methyl ester was the most abundant (84.05%), while tetradecanoic acid methyl ester was the least (11.79%). This study successfully used GC-MS to identify the fatty acid profile in both localities, and it can be used as a promising non-invasive biomarker strategy.

Keywords extracellular vesicles, exosomes, fatty acids, fatty acid, methyl esters

1.0. Introduction

Extracellular vesicles (EVs) are nanosized vesicles secreted by both eukaryotic and prokaryotic cells (Woith et al., 2019) functioning as intercellular communication tools (Park et al., 2023). These vesicles carry biological cargo such as proteins, lipids, glycans, and nucleic acids that reflect the physiological state of their parent cells (Welsh et al., 2020). EVs are abundantly found in bodily fluids like urine (Park et al., 2023), saliva (Han et al., 2022), and blood (Puhm et al., 2021) , making them an accessible target for non-invasive analysis. Recent studies have extensively explored the proteomic, lipidomic, and genomic contents of EVs, establishing their significance in differentiating between healthy and diseased individuals for conditions such as cancer (Fitts et al., 2019), autoimmune (Lu et al., 2021), and inflammatory diseases (Hwang et al., 2021).

Lipidomic and proteomic profiling have garnered significant interest in recent years for their potential to elucidate complex biological processes. These analyses are commonly performed using liquid chromatography-mass spectrometry (LC-MS), owing to its capability to handle large, polar, and thermally labile biomolecules such as lipids and nucleotides. However, LC-MS faces notable challenges in sensitivity and selectivity, particularly due to the structural complexity of analytes and the presence of isobaric and isomeric species (De Girolamo et al., 2022). In contrast, gas chromatography-mass

spectrometry (GC-MS) offers superior resolution and separation efficiency for small, volatile, and thermally stable molecules, such as fatty acids and their methyl esters (FAMEs) (Chiu & Kuo, 2020). Given these advantages, GC-MS was selected in the present study as the analytical platform of choice to achieve high-resolution profiling of small lipid molecules. Fatty acids can be derivatized into FAMEs and efficiently separated using GC-MS (Ostermann et al., 2014). However, their application in EV research remains significantly understudied. Out of 83 studies retrieved using the keyword 'fatty acid in EVs' on Scopus, only one focused on using fatty acids as a profiling medium, highlighting a significant gap in the field in early 2024.

EVs consist of three main subtypes: exosomes, microvesicles, and apoptotic bodies, each differing in biogenesis, size, and cargo (Hadizadeh et al., 2022). These vesicles contribute to various physiological processes, including immune regulation, organ homeostasis, and disease progression. Exosomes, due to their nano-size (30-150 nm) and ability to cross the blood-brain barrier, are also being studied for therapeutic applications like drug delivery (Haney et al., 2015). This characteristic of exosomes also shows its potential for use as a disease biomarker (Jalaludin et al., 2023). In this study, fatty acids were isolated from urinary EVs to identify their profile after derivatization. This fatty acid profile identification was also based on the locality of the urine sample, i.e., EV luminal space and urine. As shown in limited liver studies, the fatty acid profiling in EVs has proven effective in distinguishing disease states, suggesting a promising and selective approach for non-invasive diagnostics that are yet to be applied to urinary EVs based on their locality.

2.0. Materials and methods

2.1. Materials

The chemicals and reagents used in this study were obtained from the following suppliers: Dithiothreitol (DTT), protease inhibitor, BCA Protein Assay Kit, Phosphate Buffered Saline (PBS), Radioimmunoprecipitation Assay Buffer (RIPA), and Trimethylsilyl diazomethane (TMS-DM) were purchased from SolarBio. Methyl-tert-butyl ether (MTBE) and butylated hydroxy toluene (BHT) were obtained from Macklin, while methanol and glacial acetic acid were sourced from MHBG. Hydrochloric acid was purchased from Sigma Aldrich, and n-hexane was acquired from Bendosen. The fatty acid standards, which are oleic acid (99%) and palmitic acid (99%), were obtained from Sigma Aldrich.

2.2. Sample collection and preparation

A freshly collected morning urine sample was collected from a volunteer (n=6) after the consent form was given prior to urine sample collection (Thomas et al., 2010). The collected urine was pooled and treated by adding 0.30 ml of protease inhibitor and 0.1874 g of dithiothreitol (DTT) (Street et al., 2017).

2.3. Extracellular vesicles isolation

Urine samples were subjected to sequential centrifugation and ultracentrifugation to isolate EVs. Initially, 50 mL Falcon tubes containing treated urine were centrifuged at 2,000 × g for 30 minutes at 4°C using a Beckman Coulter Allegra X-15R centrifuge to remove cell debris. The supernatant was collected, and the pellet discarded (Erdbrügger et al., 2021). The supernatant underwent ultracentrifugation at an average of 17,000 × g (maximum 23,800 × g) for 15 minutes at 4°C using a Thermo Scientific wX Ultra Series centrifuge to remove residual debris and large vesicles.

A second ultracentrifugation was performed at an average of 200,000 × g (maximum 281,200 × g) for 1 hour at 4°C to pellet the EVs (Witwer et al., 2013). The supernatant from the first ultracentrifugation cycle was diluted with 15 mL PBS and subjected to a second identical ultracentrifugation cycle to optimize recovery. The resulting EV pellets from both cycles were resuspended in 100 µL of 1× PBS and stored at −80°C. Before analysis, samples were rapidly thawed in a 37°C water bath for 3 seconds with agitation. Repeated freeze-thaw cycles were avoided to preserve vesicle integrity.

2.4. Particle size analyzer

EVs' size distribution by number, intensity and volume was measured using a Particle Size Analyzer (PSA), Malvern Mastersizer 3000. Blue lasers with a wavelength of 488 nm were used in this analysis. First, the sample was quickly thawed by repeated 3-second dipping with shaking in a 37°C water bath. Next, samples were diluted to 10 mL with PBS at a ratio of 1:300 for suitability in the instrument. The PSA instrument maintained temperature at 4°C to avoid EV degradation. Three replicates of each size distribution were run. The sample was discarded after being analyzed, and the results were recorded (Street et al., 2017).

2.5. Protein quantification

The protein concentration of the EVs was measured using the Solarbio BCA Protein Assay Kit. The BCA assay was conducted according to the manufacturer's instructions. BCA working solution and bovine serum albumin (BSA) standard working solution were prepared according to the protocol. 0, 2, 4, 6, 8, 12, 16, 20 µl of BSA standard working solution (0.5mg/ml) were added to the well plates. Samples were thawed before the assay. 1-cycle sample was diluted to 12× dilution factors, 2-cycle sample was diluted to 7× dilution factors, while the control (non-centrifuged urine sample) was diluted to 15× dilution factors. The absorbance was measured using BMG Labtech Spectrostar Nano Microplate Reader at wavelength 562 nm, and a standard curve was plotted to calculate protein sample content (Park et al., 2023).

2.6. Fatty acid derivatization

EV samples were chemically lysed to release the fatty acid content within the luminal space, by using radioimmunoprecipitation (RIPA) buffer at a 1:1 ratio and incubated for 30 minutes at 4°C (Shehadul Islam et al., 2017). Next, released fatty acids were extracted by adding 5 mL methyl-tert-butyl-ether (MTBE) with 200µL lysis and incubated with a shaker for 1 hour at room temperature (Saini et al., 2021). 1.25 mL ultrapure is added and centrifuged at 1000 x g for 10 minutes. 10:3:2.5 of MTBE: methanol: ultrapure water was added, and the upper layer was collected and dried. next, the fatty acids extracted are derivatized with trimethylsilyl-diazomethane (TMS-DM) (Salimon et al., 2014). TMS-DM was added in molar excess of 2 M n-hexane (100 µL) at 50°C. A few drops of glacial acetic acid were added until the yellow colour disappeared to remove any unreacted TMS-DM. The mixture was diluted with 1 ml of 0.5% NaCl solution. 1 ml of n-hexane (containing 50 ppm BHT) was added. Two layers of the mixture were observed, and the upper layer containing derivatized fatty acid was collected.

2.7. GC analysis

Agilent Technologies' GC7890A Gas Chromatography apparatus with an HP5-MS column was used for analysis. The column initial temperature was 70°C, held for 1 minute, and increased to a final temperature of 325°C at 6.25°C per minute. Helium gas carrier was used at a flow rate of 0.9 ml/min. mass condition is recorded at electron energy 70 EV with mass range 40-650 AMU (Tan et al., 2020).

3.0. Results and discussion

3.1. Evaluation of protein removal in EV isolation

A standard working solution with known protein concentration was prepared according to the protocol. From the absorbance, a standard curve of concentration against absorbance was plotted. The correlation coefficient, R^2, was calculated, giving the value of 0.9953, indicating a well-fit regression of known concentration to the absorbance as shown in Figure 1. The accuracy and precision data from the calibration curve obtained are shown in Table 1. The limit of detection (LOD) and limit of quantification (LOQ) obtained were 0.05995 mg/mL and 0.18168 mg/mL, respectively. Hence, the linear equation was used to calculate the protein concentration of the sample.

Table 1: Accuracy and precision analysis at the three calibration curve points of the BSA assay

Calibration curve point	Point value	Percentage of recovery (%)	Precision (RSD)
Lowest	0.05	99.63	0.0432
Middle	0.15	99.50	0.0399
Highest	0.5	97.43	0.0223

From the linear equation y = 1.0184x – 0.0006, the protein concentration is calculated and depicted in Figure 1. To test whether there is a significant loss of protein between the sample and control, a t-test statistical analysis was carried out. At a significance level of 95% (α = 0.05), the p-value is lower than α, leading to the rejection of the null hypothesis. Thus, there is a significant difference in protein concentration between the control and sample. The depletion of protein with increasing cycles indicates that ultracentrifugation effectively removes higher-density proteins retained in the sample. These proteins are suspected to be non-tetraspanins, such as albumin and uromodulin. The high-density proteins need to be removed to ensure the purity of the EVs obtained, as well as to prevent analytical interference. This occurs because high-density proteins, such

as albumins, uromodulin, and immunoglobulins that are common in urine, can obscure the detection of EV-specific protein markers such as tetraspanins, TSG-101, and ALIX. Thus, the non-EV-specific protein markers were successfully removed from the sample after two cycles of isolation.le after two cycles of isolation.

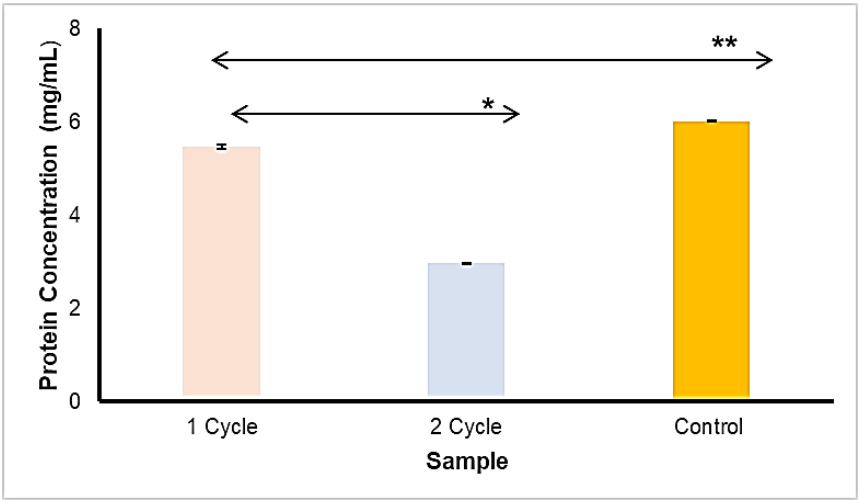

Figure 1: Protein concentration of isolation samples (1-cycle and 2-cycle) and control.

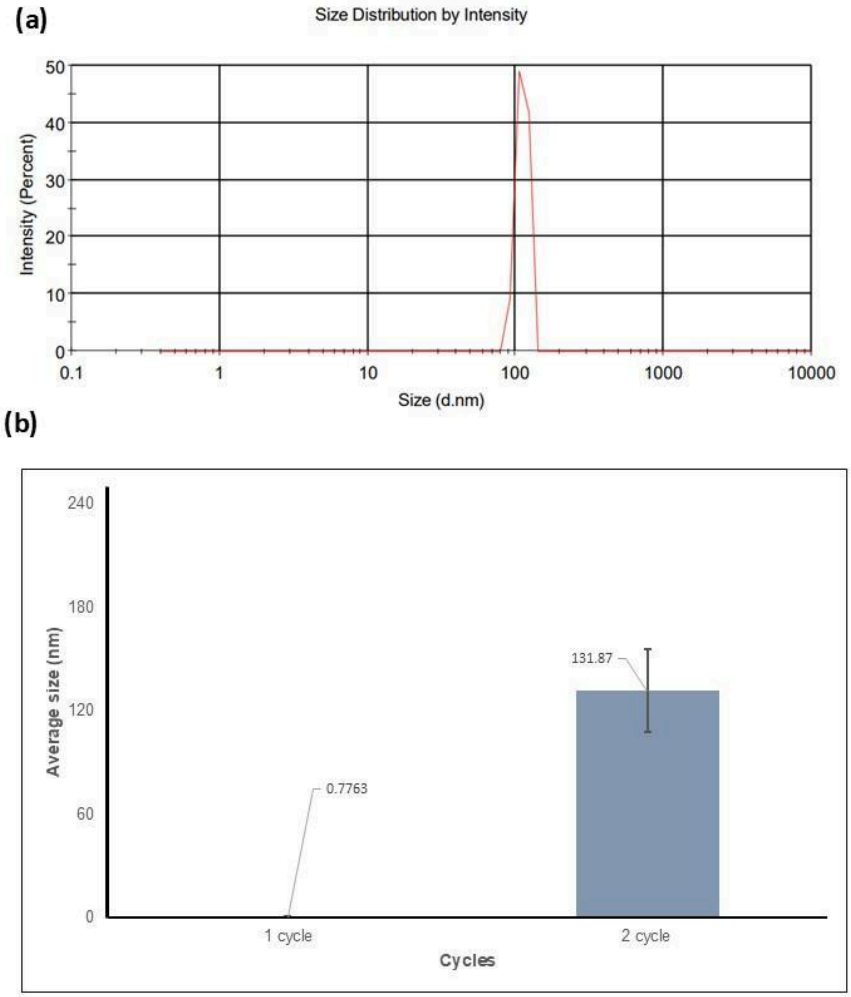

Figure 2: Particle size analysis: (a) size distribution of EVs and (b) average size by number of each cycle

3.2. Determination of EV for isolation optimization

The Malvern Mastersizer 3000 instrument determined EVs' average size (nm) for both isolation cycles. Size distribution by number was chosen as a parameter to determine the EVs particle size instead of size distribution by volume or intensity, as the latter are more sensitive to larger particles and may mask the presence of smaller ones (Burgess et al., 2004). Figures 2 (a) and 2 (b) depict the size distribution of the 2-cycle isolation.

Based on Figure 2, 2-cycles were in the desired range of exosome (30-150 nm) (Erdbrügger et al., 2021). Figure 2 (a) shows a higher peak around a 100 nm particle size distribution. Figure 2 (b) shows a major difference in the average particle size of EVs, where the average particle size of a 1-cycle sample was less than the desired range of exosomes compared to the 2-cycle sample. Hence, the 2-cycle sample was proceeded with a derivatization step. From the figure, we can conclude that increasing the cycle of ultracentrifugation can optimize EV isolation.

3.3. Gas chromatography mass spectrometer analysis of FAME

Fatty acids isolated from a urine sample as a control were extracted and derivatized, while the isolated EVs underwent cell lysis to release free fatty acids within the luminal space. The extracted fatty acids were then methylated with TMS-DM to form FAME for GC-MS analysis. Figure 3 shows the chromatograms of fatty acids from luminal EVs and urine control.

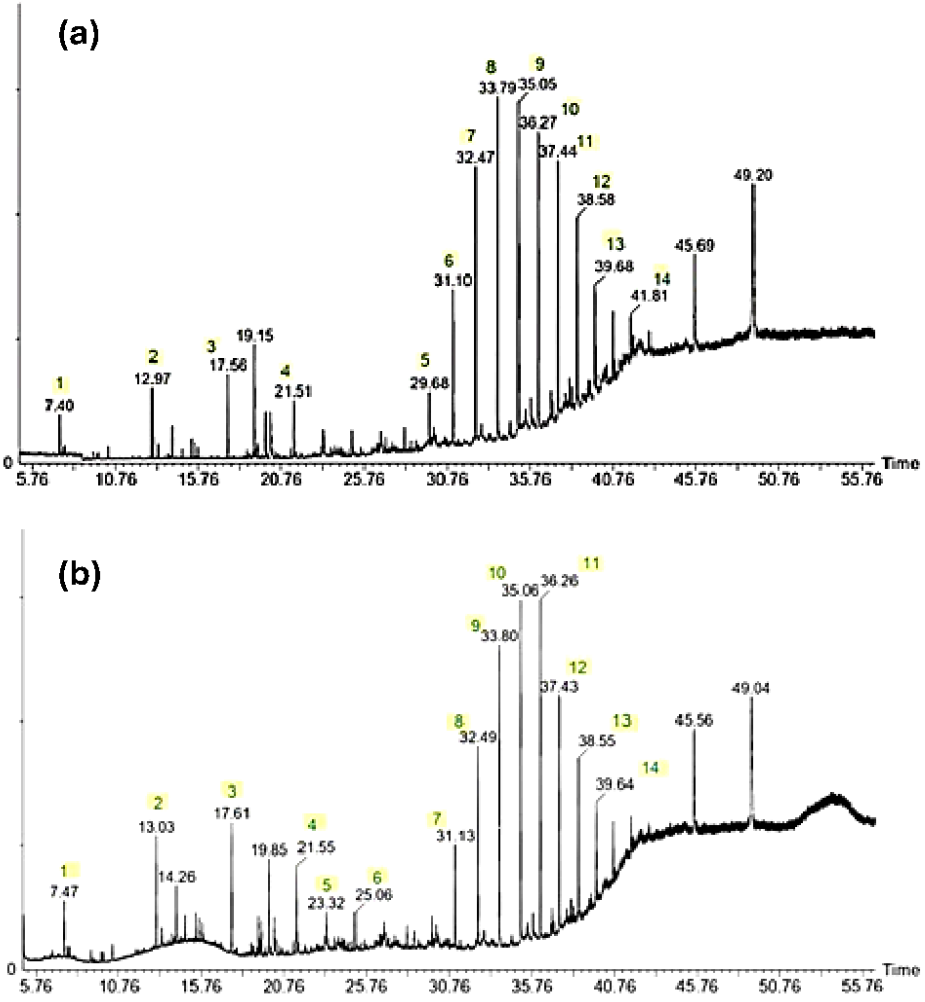

Figure 3: Fatty acid profiles of (a) EV luminal space and (b) urine

A total of 16 species of FAME were detected in both localities. Among them, three were unique and not commonly shared: tetradecanoic acid methyl ester (14:0), octadecanoic acid methyl ester (18:0), and triacontanoic acid methyl ester (30:0). Table 2 details all 16 fatty acid species detected in this study. Some fatty acid species (after peak 14) in the

chromatogram were below the detection limit, implying that the signals-to-noise ratio for this specific peak was not strong enough to be reliably quantified. The FAME were identified based on their m/z spectra. This FAME is one of the volatile organic compounds that can be found in urine (Wu et al., 2024). This peak should appear around 24.84 retention time near tetradecanoic acid methyl ester and pentadecanoic acid methyl ester retention time (Mező et al., 2022).

For the GC-MS procedure, the urine sample was diluted five-fold before extraction to ensure that the analyzed FAME was within the optimal range of the GC-MS instrument, as shown in Figure 4. Consequently, the relative abundance of fatty acids in the urine sample was higher than in the EV luminal space. This difference may be due to several hypothetical factors, such as the fatty acid composition in human urine is highly influenced by dietary intake of volunteers (Walsh et al., 2014). Meanwhile, the composition of fatty acids in the EV luminal space reflected the lipid cargo taken up during membrane budding from the parent cells (Hadizadeh et al., 2022).

Hence, urine samples are rich with EVs released by cells in organs around the urinary system, such as the liver (hepatocyte cell) and the kidney (epithelial cell). The distinct sources of fatty acids in both localities contribute to their fatty acid composition (Hadizadeh et al., 2022). As shown in Figure 4, the most abundant fatty acid species in the EV luminal space was lignoceric acid (24:0), a fatty acid commonly found in cells due to its role in the formation of sphingolipids and ceramide, which are essential for cell structure and stability of the parent cell.

Table 2: 16 FAME species found in luminal space and urine control

Peak no.	Fatty acid methyl ester species	Retention time (min)	m/z	m/z indicator
1	Heptanoic acid methyl ester ($C_6H_{13}COOHCH_3$)	7.40	144	144, 114, 84
2	Nonanoic acid methyl ester ($C_8H_{17}COOHCH_3$)	12.97	172	172, 141, 112
3	Undecanoic acid methyl ester ($C_{10}H_{21}COOHCH_3$)	17.56	200	200, 169, 140
4	Tridecanoic acid methyl ester ($C_{12}H_{25}COOHCH_3$)	21.51	228	228, 197, 168
5 (luminal)	Octadecanoic acid methyl ester ($C_{17}H_{35}COOHCH_3$)	29.68	298	298, 264, 238
5 (urine)	Tetradecanoic acid methyl ester ($C_{13}H_{25}COOHCH_3$)	23.32	242	242, 210, 180
6 (luminal)	Heneicosanoic acid methyl ester ($C_{20}H_{41}COOHCH_3$)	31.10	311	311, 281, 267
6 (urine)	Pentadecanoic acid methyl ester (C14H29COOHCH3)	25.06	256	256, 224, 195
7	Docosanoic acid methyl ester ($C_{21}H_{43}COOHCH_3$)	32.47	325	325, 296, 281
8	Tricosanoic acid methyl ester ($C_{22}H_{45}COOHCH_3$)	33.79	339	339, 310, 281
9	Tetracosanoic acid methyl ester ($C_{23}H_{47}COOHCH_3$)	35.05	353	353, 323, 309
10	Pentacosanoic acid methyl ester ($C_{24}H_{49}COOHCH_3$)	36.27	367	368, 337, 327
11	Hexacosanoic acid methyl ester ($C_{25}H_{53}COOHCH_3$)	37.434	381	352, 337
12	Heptacosanoic acid methyl ester ($C_{26}H_{55}COOHCH_3$)	38.58	395	394, 365, 352
13	Octacosanoic acid methyl ester ($C_{27}H_{57}COOHCH_3$)	39.68	409	409, 378, 365
14	Triacontanoic acid methyl ester ($C_{29}H_{59}COOHCH_3$)	41.81	437	437, 406, 379

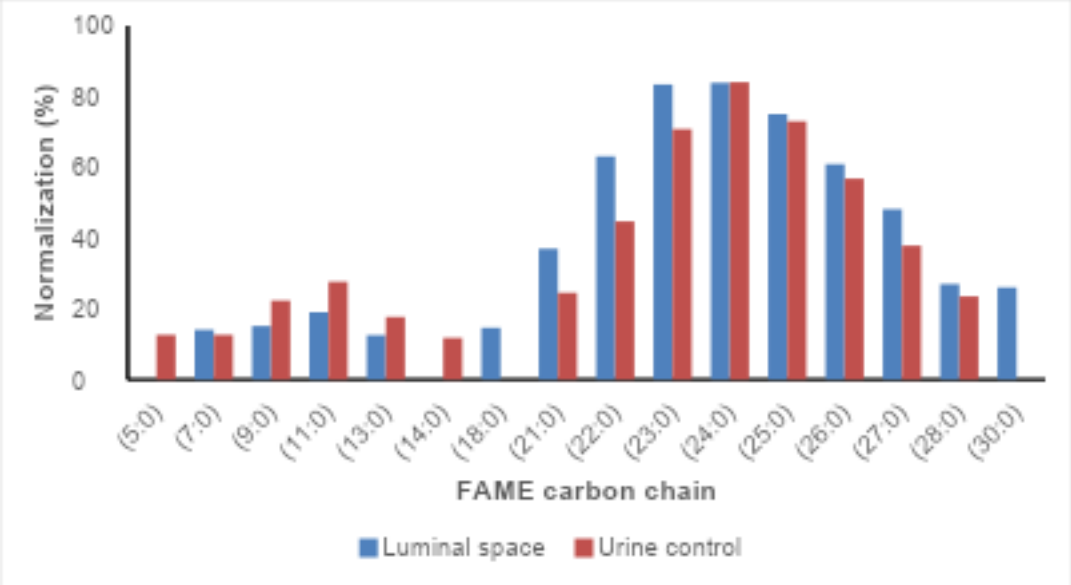

Figure 4: Comparison of FAME profiles between luminal space and urine control EVs. Normalization (%) values represent the relative abundance of each FAME species based on their carbon chain lengths, ranging from C5:0 to C30:0.

4.0. Conclusion

The study successfully optimized EVs isolation by incorporating a second cycle in ultracentrifugation. This is demonstrated by the resulting size of particles of both cycles of isolation, with values of 0.7763 nm for the 1-cycle and 131.87 nm for the 2-cycle isolation. Fatty acids were successfully derivatized into FAME species by reaction with TMS-DM. 16 FAME species were detected in both localities, with lignoceric acid (24:0) being the most abundant. The urine samples showed a higher abundance of fatty acids than the EVs luminal space, possibly due to the dietary intake of the volunteers. Fatty acid profiling and the analysis of species abundance between localities in the EVs urine sample were successfully conducted using selective derivatization with TMS-DM. The novel findings from this research may contribute to the further study of fatty acids as disease biomarkers as a selective, advanced and direct method compared to traditional lipidomic and proteomic EVs analysis.

Acknowledgment

This research was supported by Universiti Teknologi Malaysia, UTM-Encouragement Research Grant (Q.J130000.3854.31J99).

References

Aitekenov, S., Gaipov, A., & Bukasov, R. (2021). Review: Detection and quantification of proteins in human urine. *Talanta, 223*(1), 121718. https://doi.org/10.1016/j.talanta.2020.121718

Burgess, D. J., Duffy, E., Etzler, F., & Hickey, A. J. (2004). Particle size analysis: AAPS workshop report, cosponsored by the Food and Drug Administration and the United States Pharmacopeia. *The AAPS Journal, 6*(3), 20. https://doi.org/10.1208/aapsj060320

Chiu, H.-H., & Kuo, C.-H. (2020). Gas chromatography-mass spectrometry-based analytical strategies for fatty acid analysis in biological samples. *Journal of Food and Drug Analysis, 28*(1), 60–73. https://doi.org/10.1016/j.jfda.2019.10.003

De Girolamo, A., Lippolis, V., & Pascale, M. (2022). Overview of recent liquid chromatography mass spectrometry-based methods for natural toxins detection in food products. *Toxins, 14*(5), 50328. https://doi.org/10.3390/toxins14050328

Erdbrügger, U., Blijdorp, C. J., Bijnsdorp, I. V., Borràs, F. E., Burger, D., Bussolati, B., Byrd, J. B., et al. (2021). Urinary extracellular vesicles: A position paper by the Urine Task Force of the International Society for Extracellular Vesicles. *Journal of Extracellular Vesicles, 10*(7), e12093. https://doi.org/10.1002/jev2.12093

Fitts, C. A., Ji, N., Li, Y., & Tan, C. (2019). Exploiting exosomes in cancer liquid biopsies and drug delivery. *Advanced Healthcare Materials, 8*(6), e1801268. https://doi.org/10.1002/adhm.201801268

Hadizadeh, N., Bagheri, D., Shamsara, M., Hamblin, M. R., Farmany, A., Xu, M., Liang, Z., Razi, F., & Hashemi, E. (2022). Extracellular vesicles biogenesis, isolation, manipulation and genetic engineering for potential in vitro and in vivo therapeutics: An overview. *Frontiers in Bioengineering and Biotechnology, 10*, 1019821. https://doi.org/10.3389/fbioe.2022.1019821

Han, P., Bartold, P. M., & Ivanovski, S. (2022). The emerging role of small extracellular vesicles in saliva and gingival crevicular fluid as diagnostics for periodontitis. *Journal of Periodontal Research, 57*(1), 219–231. https://doi.org/10.1111/jre.12950

Haney, M. J., Klyachko, N. L., Zhao, Y., Gupta, R., Plotnikova, E. G., He, Z., Patel, T., Piroyan, A., Sokolsky, M., Kabanov, A. V., & Batrakova, E. V. (2015). Exosomes as drug delivery vehicles for Parkinson's disease therapy. *Journal of Controlled Release, 207*, 18–30. https://doi.org/10.1016/j.jconrel.2015.03.033

Hwang, H. S., Kim, H., Han, G., Lee, J. W., Kim, K., Kwon, I. C., Yang, Y., & Kim, S. H. (2021). Extracellular vesicles as potential therapeutics for inflammatory diseases. *International Journal of Molecular Sciences, 22*(11), 5487. https://doi.org/10.3390/ijms22115487

Jalaludin, I., Nguyen, H. Q., Jang, K. S., Lee, J., Lubman, D. M., & Kim, J. (2023). Matrix-assisted laser desorption/ionization-Fourier-transform ion cyclotron resonance-mass spectrometry analysis of exosomal lipids from human serum. *Rapid Communications in Mass Spectrometry, 37*(2), e9427. https://doi.org/10.1002/rcm.9427

Kim, T. K. (2015). T test as a parametric statistic. *Korean Journal of Anesthesiology, 68*(6), 540–546. https://doi.org/10.4097/kjae.2015.68.6.540

Lu, M., DiBernardo, E., Parks, E., Fox, H., Zheng, S.-Y., & Wayne, E. (2021). The role of extracellular vesicles in the pathogenesis and treatment of autoimmune disorders. *Frontiers in Immunology, 12*, 566299. https://doi.org/10.3389/fimmu.2021.566299

Mező, E., Hartmann-Balogh, F., Madarászné Horváth, I., Bufa, A., Marosvölgyi, T., Kocsis, B., & Makszin, L. (2022). Effect of culture conditions on fatty acid profiles of bacteria and lipopolysaccharides of the genus Pseudomonas—GC-MS analysis on ionic liquid-based column. *Molecules, 27*(20), 6930. https://doi.org/10.3390/molecules27206930

Ostermann, A. I., Müller, M., Willenberg, I., & Schebb, N. H. (2014). Determining the fatty acid composition in plasma and tissues as fatty acid methyl esters using gas chromatography – A comparison of different derivatization and extraction procedures. *Prostaglandins, Leukotrienes and Essential Fatty Acids, 91*(6), 235–241. https://doi.org/10.1016/j.plefa.2014.10.002

Park, S., Jalaludin, I., Hwang, H., Ko, M., Adelipour, M., Hwan, M., Cho, N., Kim, K. K., Lubman, D. M., & Kim, J. (2023). Size-exclusion chromatography for the characterization of urinary extracellular vesicles. *Journal of Chromatography B, 1228*, 123828. https://doi.org/10.1016/j.jchromb.2023.123828

Puhm, F., Boilard, E., & Machlus, K. R. (2021). Platelet extracellular vesicles: Beyond the blood. *Arteriosclerosis, Thrombosis, and Vascular Biology, 41*(1), 87–96. https://doi.org/10.1161/atvbaha.120.314644

Saini, R. K., Prasad, P., Shang, X., & Keum, Y. S. (2021). Advances in lipid extraction methods – A review. *International Journal of Molecular Sciences, 22*(24), 13643. https://doi.org/10.3390/ijms222413643

Salimon, J., Omar, T., & Salih, N. (2014). Comparison of two derivatization methods for the analysis of fatty acids and trans fatty acids in bakery products using gas chromatography. *The Scientific World Journal, 2014*, A906407. https://doi.org/10.1155/2014/906407

Shehadul Islam, M., Aryasomayajula, A., & Selvaganapathy, P. R. (2017). A review on macroscale and microscale cell lysis methods. *Micromachines, 8*(3), 83. https://doi.org/10.3390/mi8030083

Street, J. M., Koritzinsky, E. H., Glispie, D. M., & Yuen, P. S. T. (2017). Urine exosome isolation and characterization. In J.-C. Gautier (Ed.), *Drug Safety Evaluation: Methods and Protocols* (pp. 413–423). Springer. https://doi.org/10.1007/978-1-4939-7172-5_23

Tan, B., Zhang, Y., Zhang, T., He, J., Luo, X., Bian, X., Wu, J., Zou, C., Wang, Y., & Fu, L. (2020). Identifying potential serum biomarkers of breast cancer through targeted free fatty acid profiles screening based on a GC-MS platform. *Biomedical Chromatography, 34*(10), e4922. https://doi.org/10.1002/bmc.4922

Thomas, C. E., Sexton, W., Benson, K., Sutphen, R., & Koomen, J. (2010). Urine collection and processing for protein biomarker discovery and quantification. *Cancer Epidemiology, Biomarkers & Prevention, 19*(4), 953–959. https://doi.org/10.1158/1055-9965.EPI-10-0069

Walsh, M. C., McLoughlin, G. A., Roche, H. M., Ferguson, J. F., Drevon, C. A., Saris, W. H., Lovegrove, J. A., Risérus, U., López-Miranda, J., Defoort, C., Kieć-Wilk, B., Brennan, L., & Gibney, M. J. (2014). Impact of geographical region on urinary metabolomic and plasma fatty acid profiles in subjects with the metabolic syndrome across Europe: The LIPGENE study. *British Journal of Nutrition, 111*(3), 424–431. https://doi.org/10.1017/S0007114513002602

Welsh, J. A., van der Pol, E., Bettin, B. A., Carter, D. R. F., Hendrix, A., Lenassi, M., Langlois, M. A., Llorente, A., van de Nes, A. S., Nieuwland, R., Tang, V., Wang, L., Witwer, K. W., & Jones, J. C. (2020). Towards defining reference materials for measuring extracellular vesicle refractive index, epitope abundance, size and concentration. *Journal of Extracellular Vesicles, 9*(1), 1816641. https://doi.org/10.1080/20013078.2020.1816641

Witwer, K. W., Buzas, E. I., Bemis, L. T., Bora, A., Lasser, C., Lotvall, J., Nolte-'t Hoen, E. N., Piper, M. G., Sivaraman, S., Skog, J., Thery, C., Wauben, M. H., & Hochberg, F. (2013). Standardization of sample collection, isolation and analysis methods in extracellular vesicle research. *Journal of Extracellular Vesicles, 2*, 20360. https://doi.org/10.3402/jev.v2i0.20360

Woith, E., Fuhrmann, G., & Melzig, M. F. (2019). Extracellular vesicles – Connecting kingdoms. *International Journal of Molecular Sciences, 20*(22), 5695. https://doi.org/10.3390/ijms20225695

Wu, H. H. L., Possell, M., Nguyen, L. T., Peng, W., Pollock, C. A., & Saad, S. (2024). Evaluation of urinary volatile organic compounds as a novel metabolomic biomarker to assess chronic kidney disease progression. *BMC Nephrology, 25*(1), 352. https://doi.org/10.1186/s12882-024-03819-0